Infrared studies of the interaction of carbon monoxide and dinitrogen with ferrisilicate MFI-type zeolites

A. Zecchina [1], F. Geobaldo [2], C. Lamberti, S. Bordiga

Dipartimento di Chimica Inorganica, Chimica Fisica e Chimica dei Materiali, Università di Torino, Via P. Giuria 7, 10125 Turin, Italy

G. Turnes Palomino and C. Otero Areán [1]

Departamento de Química, Universidad de las Islas Baleares, 07071 Palma de Mallorca, Spain

Received 5 June 1996; accepted 1 August 1996

Fourier transform IR spectroscopy of CO and N_2, adsorbed at liquid nitrogen temperature, was used to characterize an MFI-type H-FeZSM-5 ferrisilicate which was synthesized with a Si/Fe ratio of 50. Thermal treatment of this material at 773 and 973 K was performed in order to follow formation of extraframework species. On samples fired at 773 K Brønsted acid sites were present which gave an O–H stretching band at 3630 cm^{-1}. These hydroxyl groups formed adducts with both probe molecules, which were monitored by the corresponding bathochromic shift, $\Delta\nu$. Corresponding values for adsorbed CO and N_2 were $\Delta\nu = -270$ and $\Delta\nu = -100$, respectively. Increasing the firing temperature up to 973 K led to complete removal of iron from the zeolite framework, and consequent disappearance of Brønsted acidity. In this process, extraframework iron oxide species were formed which were also characterized by IR spectroscopy of the adsorbed probe molecules. Both CO and N_2 gave Lewis-type adducts with coordinatively unsaturated Fe^{3+} ions present in the extraframework material. A comparison is made with results of a previous study on the H-GaZSM-5 isomorph.

Keywords: zeolites; ferrisilicate; H-FeZSM-5; CO adsorption; dinitrogen adsorption; IR spectroscopy

1. Introduction

Replacement of Al or Si in zeolite frameworks by heteroatoms generates new materials with significantly modified physicochemical properties. Among other uses, these materials have the potential to perform satisfactorily as highly selective catalysts for both the petrochemical industry and the synthesis of fine chemicals [1,2]. However, the preparation and characterization of zeotype materials containing framework heteroatoms often meet with experimental difficulties. In the case of iron, a major complication in the synthesis comes from the tendency of Fe^{3+} ions to hydrolyse and form aggregates of iron oxides and oxohydroxides in alkaline aqueous solutions. Despite this complication many molecular sieve ferrisilicates have been prepared; among them the analogues of the zeolites sodalite [3], faujasite [4], LTL [5], mordenite [6], and ZSM-5 [7–13]. Detailed accounts were given by Szostak [14] and by Ratnasamy and Kumar [15,16].

Synthesis of ferrisilicates in the protonic form, needed for catalytic applications, is usually accomplished [8,12,17] starting from the Fe-doped sodium form which is then ion exchanged with NH_4^+ and heated at about 800 K to render the H^+ form. Alternatives are the fluoride route [15,18] and synthesis in alcoholic solutions [19,20] both of which can yield directly the ammonium form and minimize the risk of forming insoluble iron oxides during early stages of the preparation procedure.

There is conclusive evidence [14,15,21] that, when carefully synthesized, Fe^{3+} ions occupy tetrahedral lattice sites in MFI-type ferrisilicates, i.e., they isomorphously substitute for silicon in the as-synthesized materials. However, subsequent thermal treatments (needed for template burning and for conversion of the ammonium into the protonic form) can lead to local disruption of the silicate framework with attendant formation of extraframework iron species. These are small aggregates of iron oxides (or oxohydroxides) which remain trapped inside the zeolite channels and can act as catalytic centres, either independently or in synergy with protonic (Brønsted acid) sites. MFI-type ferrisilicates are known to show catalytic activity in a number of chemical processes, such as xylene isomerization (with para selectivity), toluene alkylation, shape selective oxidation of hydrocarbons [22–28], dehydrogenation of alkylbenzenes to (substituted) styrenes [29], and reduction of nitric oxide by hydrocarbons [30]. Presence of iron species appears to be an important factor in all of these processes. Thus, FeZSM-5 zeolites are very active in the selective oxidation of benzene to phenol (when N_2O is the source of oxygen), while other metals (Ti, Cr,

[1] To whom correspondence should be addressed.

[2] Also at: Dipartimento di Scienza dei Materiali e Ingegneria Chimica, Politecnico di Torino, Turin, Italy.

Mn, Ni, Cu) introduced in ZSM-5 are not catalytically active in this reaction [27]. Similarly, H-FeZSM-5 is much more active [31,32] than other metallosilicates for the catalytic reduction of NO by hydrocarbons.

A key factor for understanding catalytic processes mediated by ferrisilicates is a detailed characterization of the material, with particular emphasis on iron species. The purpose of the present work was to study Brønsted and Lewis acid sites in H-FeZSM-5, paying special attention to extraframework species formed during template removal and thermal activation. This is particularly relevant to catalytic processes where under steaming conditions part of the iron is removed from the zeolite framework and forms finely divided iron oxide particles. Characterization of the materials under study was carried out by mid-IR spectrometry of adsorbed dinitrogen and carbon monoxide. The use of these diatomic molecules as spectroscopic probes for IR studies of zeolites was discussed elsewhere [33–35], and their relative merits were also analysed. The present work completes a recent study of the same H-FeZSM-5 material which was performed using other spectroscopic techniques, mainly UV–vis and EPR spectroscopies, EXAFS and XANES [36,37].

2. Materials and methods

Details on the synthesis of the H-FeZSM-5 sample used as the starting material for the present study were given elsewhere [38]. Briefly, ethanolic solutions of $FeCl_3$ and tetraethyl orthosilicate were mixed and stirred for 30 min, then tetrapropylammonium hydroxide was added as the templating agent and the resulting solution was heated to 353 K and held for 5 h before being transferred into an autoclave (with Teflon lining) and heated under autogenous pressure for 140 h at 443 K; the resulting solid product was thoroughly washed with distilled water and dried in air at 393 K. X-ray diffraction analysis showed a single crystalline phase with ZSM-5 topology, structure type MFI in the IUPAC nomenclature [39]. This orthorhombic phase had a unit cell volume of 5379 $Å^3$, which suggests incorporation of iron into the zeolite framework since the corresponding value for MFI-type silicalite is 5344 $Å^3$ [14]. Further evidence for iron incorporation is provided by previous results from UV–vis and EXAFS spectroscopies [37] which showed the presence in the as-synthesized material of tetrahedrally coordinated Fe^{3+} ions having an Fe–O bond distance of 1.85 Å. No evidence for octahedrally coordinated Fe^{3+} ions was found [37]. Elemental analysis gave a value of 50 for the Si/Fe ratio, which was consistent with the composition of the parent gel.

For IR studies, portions of the as-synthesized material were made into self-supporting wafers and calcined inside an IR cell at 773 K to accomplish template burning, which was monitored by the disappearance of the C–H stretching bands in the 2850–3100 cm^{-1} region. The IR cell was then outgassed in a dynamic vacuum (residual pressure < 10^{-4} Torr) for 1 h at 673 K, before dosing with CO or N_2. In order to investigate formation of extraframework species as a function of thermal treatment, the temperature of some of the wafers was further raised (slowly) in air up to 973 K prior to outgassing for 1 h at 673 K in vacuum. Low-temperature transmission IR spectra were recorded, at 2 cm^{-1} resolution, on a Bruker IFS 66 FTIR spectrometer. Although the IR cell was permanently cooled with liquid nitrogen during acquisition of spectra, the actual sample temperature (under the IR beam) was likely to be about 100–110 K.

3. Results and discussion

3.1. IR spectra in the O–H stretching region

Fig. 1 (full line spectrum) shows the O–H stretching region of the ferrisilicate sample calcined at 773 K. Three main IR absorption bands are observed at 3747, 3630, and 3475 cm^{-1}, respectively. On closer inspection, a clear shoulder at 3720 cm^{-1} is observed in the low-frequency side of the 3747 cm^{-1} band (see inset in fig. 1),

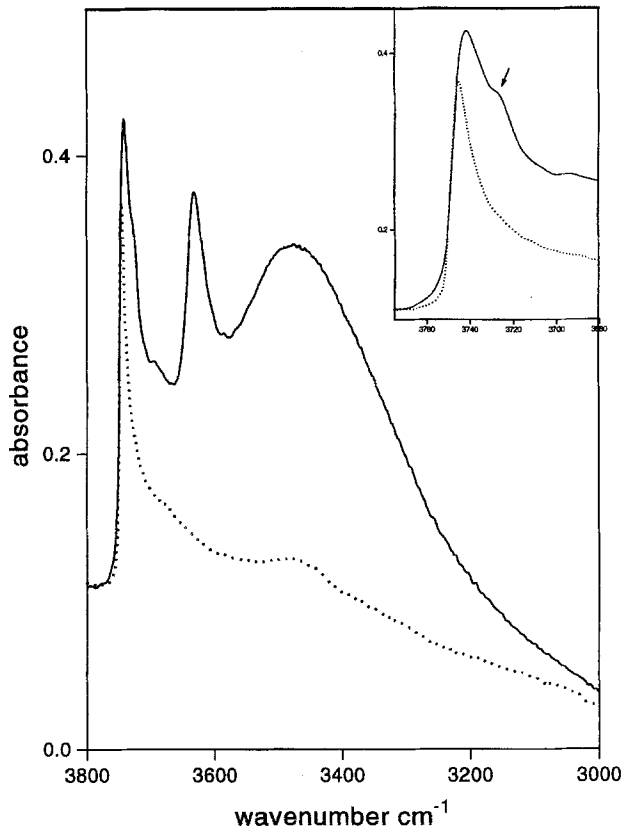

Fig. 1. Infrared spectra in the O–H stretching region of H-FeZSM-5 calcined at 773 K (full line spectrum), and at 973 K (dotted line). Inset depicts an enlarged view of the silanol band, showing the shoulder at 3720 cm^{-1}.

and also a very weak IR absorption can be noted at 3690 cm^{-1}.

The sharp band at 3747 cm^{-1} is assigned to isolated silanols which are expected to be present mainly on external surfaces of the zeolite crystals, while the shoulder at 3720 cm^{-1} is assigned to terminal SiOH groups of hydrogen-bonded silanol chains, as depicted in scheme 1. These terminal SiOH groups would occur at internal silanol nests predominantly formed when iron was removed from the zeolite framework, presumably during template burning. Hydrogen-bonded silanols in these nests give rise to the broad band observed in the 3475 cm^{-1} range. Similar features of the corresponding IR spectra were observed for highly defective silicalites and for very finely divided H-ZSM-5 samples, and detailed discussions were given elsewhere [40,41]. Interaction of hydroxyls with nearby oxygen atoms forming hydrogen-bonded OH species, which could contribute to IR absorption in the 3475 cm^{-1} region, would also occur in the neighborhood of defective sites arising from imperfect crystallization of the parent gel or in regions of amorphous material which would escape detection by X-ray diffraction. Evidence for amorphous material was found by Ulan et al. [13] in a detailed study of MFI-type iron silicates, which was carried out using transmission electron microscopy and selected area electron diffraction. It is conceivable that small micropores could exist in this amorphous material which could be blocked during thermal treatment, thus leaving occluded hydrogen-bonded OH groups very resistant to elimination.

The band at 3630 cm^{-1} corresponds to the O–H stretching mode of bridged Si(OH)Fe groups, which constitute the Brønsted acid sites of the ferrisilicate. The analogous band for H-ZSM-5 (which has Al instead of Fe) is usually found around 3609–3615 cm^{-1} [41–48], while for the gallosilicate analogue it appears at about 3617–3623 cm^{-1} [33,49–52]. This suggests that the Brønsted acid sites of the ferrisilicate are intrinsically weaker than those of the other isomorphs, which is in agreement with the much lower activity of H-FeZSM-5 for propene oligomerization, as reported by Parrillo et al. [53].

The weak IR absorption band observed at 3690 cm^{-1} is assigned to OH groups present in small clusters of iron extraframework species. However, we remark the low intensity of this band, and also the fact that the intensity of the 3630 cm^{-1} band is very much the same as

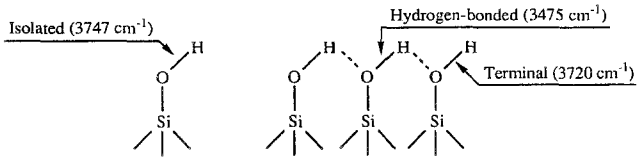

Scheme 1.

that found [33] for the corresponding Brønsted acid sites of an H-GaZSM-5 sample having a Si/Ga ratio of 50 (as in the present case for the Si/Fe ratio). Both of these facts strongly suggest that iron is mostly in the zeolite framework in the ferrisilicate sample calcined at 773 K.

Fig. 1 (dotted line spectrum) shows that increasing the calcination temperature from 773 to 973 K brings about considerable changes in the O–H stretching region. All Brønsted acid sites (band at 3630 cm^{-1}) are virtually eliminated. Severe weakening of the broad 3475 cm^{-1} band is also observed, and the 3720 cm^{-1} shoulder is no longer present: note the sharpness of the remaining 3747 cm^{-1} band. These spectral features reflect corresponding changes in the zeolite sample as follows: calcination up to 973 K causes migration of iron from framework to extraframework location with attendant elimination of Brønsted acidity; at the same time water molecules are nucleated from silanol nests and eliminated during subsequent outgassing of the zeolite wafer, thus explaining the observed disappearance of the 3720 cm^{-1} shoulder and severe weakening of the 3475 cm^{-1} band [40,41]. However, isolated silanols giving rise to the 3747 cm^{-1} band are more resistant to the thermal treatment. It is evident that the foregoing processes should cause disruption of the zeolite framework and development of Lewis acidity. Further considerations to this point are given in the following sections.

3.2. Adsorption of carbon monoxide

Upon adsorption of CO (at 77 K) on the ferrisilicate sample fired at 773 K, the band at 3630 cm^{-1} (Brønsted acid sites) is progressively eroded and a new broad band develops which has a maximum at about 3360 cm^{-1}, as shown in fig. 2. The frequency shift ($\Delta\nu = -270$ cm^{-1}) and the observed increase in line width and intensity are the classical effects of a hydrogen bonding OH···CO interaction [54], as depicted in scheme 2. For comparison, reported values of the frequency shift of acidic OH groups in H-ZSM-5 upon CO adsorption are in the −308 to −340 cm^{-1} range [41,55–57]. The smaller bathochromic shift of the bridged OH groups in H-FeZSM-5 suggests a weaker Brønsted acidity of the ferrisilicate, as already stated in section 3.1, and which is also in agreement with previous reports in the literature [49,58,59]. At high CO equilibrium pressure, the bands due to isolated and terminal silanols (3747 and 3720 cm^{-1}) are also partially eroded and shifted to 3653 and 3580 cm^{-1}, respectively, due to formation of the corresponding hydrogren-bonded SiOH···CO species.

The corresponding spectra in the C–O stretching region are shown in fig. 3. For low values of the CO equilibrium pressure, a complex IR absorption is observed in the 2135–2185 cm^{-1} range which can be resolved into four components, 2180, 2172, 2157 and 2141 cm^{-1}, as depicted in the inset of fig. 3. Comparison with recently published data for CO adsorbed on H-

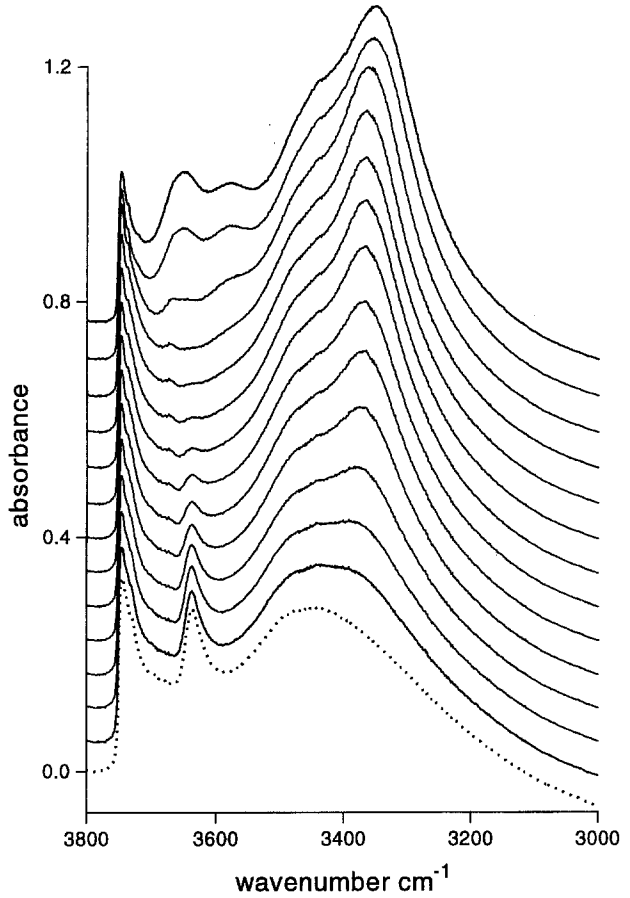

Fig. 2. Effect of increasing doses (from ca. 10^{-3} to 40 Torr) of adsorbed CO at 77 K on the O–H stretching region of H-FeZSM-5 calcined at 773 K. The dotted line spectrum corresponds to the zeolite blank. For clarity the spectra have been offset on the vertical scale.

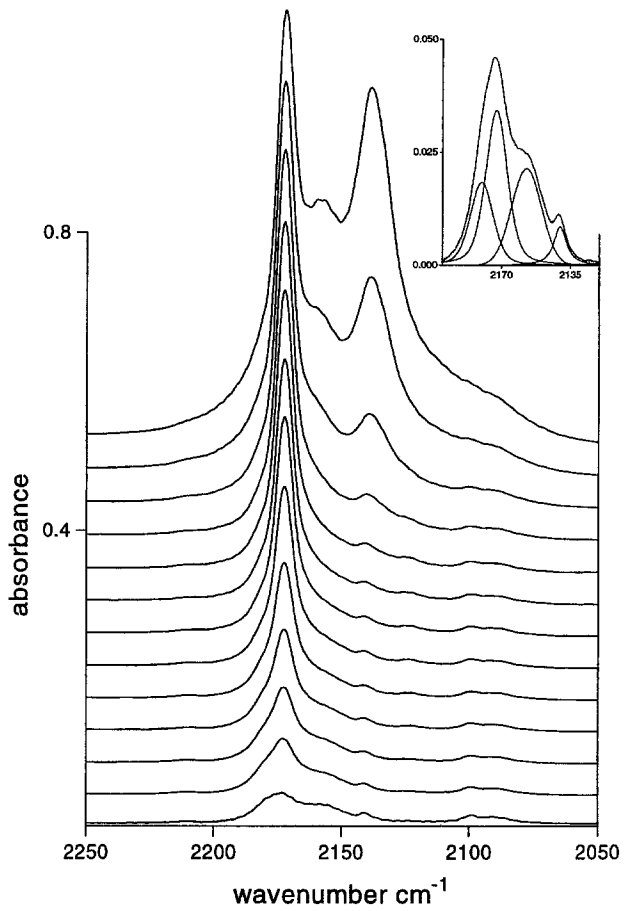

Fig. 3. Infrared spectra of CO adsorbed at 77 K and increasing equilibrium pressure (from ca. 10^{-3} to 40 Torr) on H-FeZSM-5 calcined at 773 K. All spectra were background subtracted. Inset shows computer deconvolution of the second spectrum from the bottom.

ZSM-5, H-GaZSM-5 and the protonic form of mordenite [33,41,51,60,61] leads to the unambiguous assignment of the 2172 cm^{-1} band to the CO stretching mode of the hydrogen-bonded CO adducts depicted in scheme 2. Note that, on increasing CO equilibrium pressure, this band grows in parallel with the 3360 cm^{-1} band (fig. 2), and simultaneously the O–H stretching at 3630 cm^{-1} loses intensity, thus confirming the foregoing assignment. The components at 2180 and 2157 cm^{-1}, which saturate at low CO equilibrium pressure, must correspond to species present in a very minor concentration. We assign the 2180 cm^{-1} band to the C–O stretching mode of Lewis type $Fe^{3+}\cdots CO$ adducts formed on extraframework iron oxide nanoclusters. Note that for CO adsorbed on prismatic faces of well developed α-Fe_2O_3 crystals, the corresponding IR absorption band was found in the 2165–2170 cm^{-1} range [62]. Comparison shows that extraframework iron oxide species in H-FeZSM-5 must have Fe^{3+} ions with a rather high degree of unsaturated coordination, which can act as Lewis acid sites. Assignment of the weak 2157 cm^{-1} band is more uncertain, we tentatively attribute it to CO adsorbed on coordinatively unsaturated Fe^{2+} ions formed by partial reduction of Fe^{3+} during thermal activation in vacuo of the zeolite wafer, as suggested by Raj and Sivasanker [63]. In this context, note also the weak IR absorption in the 2080–2105 cm^{-1} range (fig. 3) which was also observed for CO adsorbed on partially reduced Fe_2O_3 supported on zirconia [64]. An IR absorption band at about 2157–2160 cm^{-1} is also expected for CO interacting with silanols (see below), but this band is usually observed only at relatively high CO equilibrium pressure. Finally, the 2141 cm^{-1} band, which markedly gains intensity (and shifts to 2138 cm^{-1}) at high CO equilibrium pressure corresponds to physically adsorbed (liquid-like) CO inside the zeolite chan-

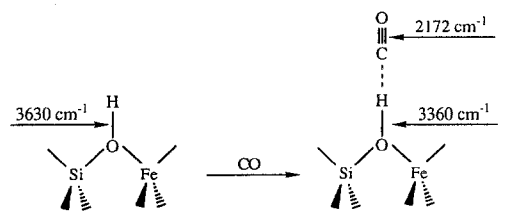

Scheme 2.

nels; it has been thoroughly discussed elsewhere [41,65] for the ZSM-5 isomorph.

CO adsorbed at 77 K on the ferrisilicate sample fired at 973 K (in which Brønsted acid sites are virtually absent) caused a gradual erosion of the free silanols band at 3747 cm^{-1}, which results shifted to 3655 cm^{-1} and considerably broadened, as shown in fig. 4. This is the expected consequence of the formation of hydrogen-bonded SiOH···CO adducts, as already stated. Further proof is provided by the (nearly) isobestic point observed at 3703 cm^{-1} in fig. 4. Note that erosion of the 3747 cm^{-1} band only develops at relatively high CO dosis, in agreement with the expected low stability of the corresponding adducts. Spectra in the C–O stretching region are shown in fig. 5. For low CO equilibrium pressure, a broad band is observed in the 2150–2200 cm^{-1} region which has main components at 2174 and at 2180 cm^{-1} (shoulder). These features are assigned to Lewis-type Fe^{3+}···CO adducts formed on extraframework iron oxide species. The band at 2174 cm^{-1}, which is close in wavenumber to that reported for CO adsorbed on well developed α-Fe_2O_3 crystals [62] is attributed to Fe^{3+}···CO species formed on extended patches of iron oxide nanoclusters, while the shoulder at 2180 cm^{-1} should correspond to more coordinatively unsaturated

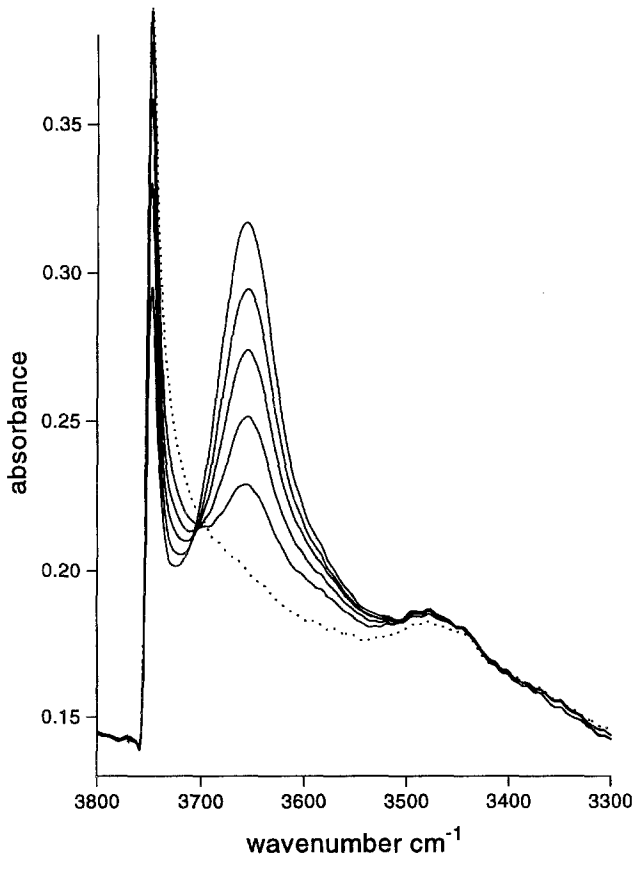

Fig. 4. Effect of increasing doses (from 1 to 40 Torr) of adsorbed CO at 77 K on the silanol band of H-FeZSM-5 calcined at 973 K. The dotted line is the zeolite blank spectrum.

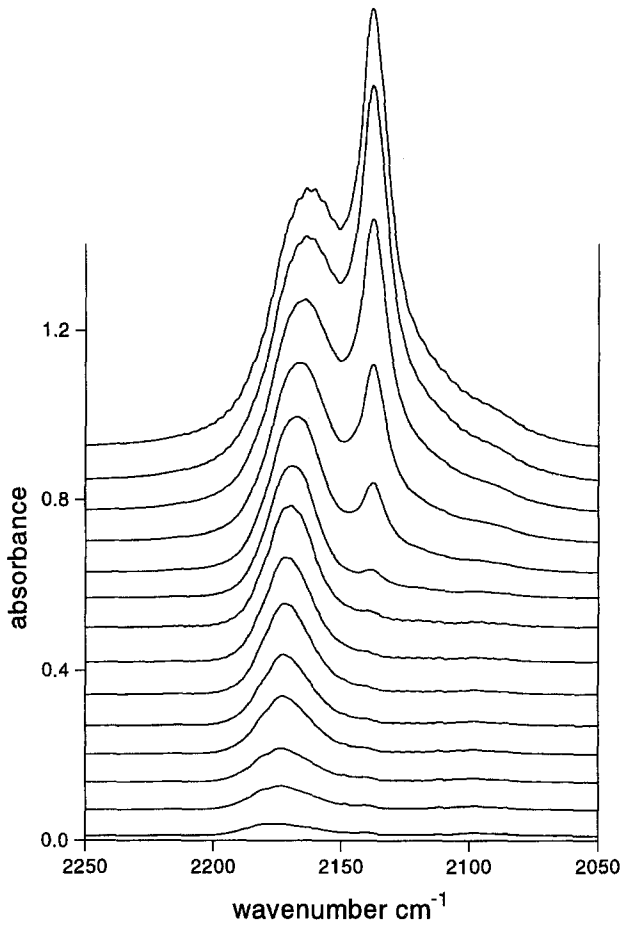

Fig. 5. Infrared spectra of CO adsorbed at 77 K and increasing equilibrium pressure (10^{-3} to 40 Torr) on H-FeZSM-5 calcined at 973 K.

Fe^{3+} ions presumably located at edges and corners of these nanoclusters. Note that this latter band was already present in the ferrisilicate sample calcined at 773 K which showed only small traces of extraframework species. Predominance of the 2174 cm^{-1} component suggests considerable aggregation of extraframework iron which was somehow unexpected for a material with such a low iron content (Si/Fe = 50). We shall return to this point after discussing dinitrogen adsorption. Note, however, that extraframework iron species can be formed not only inside the channels, but also at external surfaces of the zeolite crystals.

Fig. 5 shows that for high CO equilibrium pressure the spectra become dominated by the band at 2138 cm^{-1} corresponding to liquid-like (physisorbed) CO inside the zeolite channels. A second band is also observed at about 2160 cm^{-1} (overshadowing the weak 2174 and 2180 cm^{-1} bands discussed above); this is the C–O stretching of SiOH···CO adducts formed on silanols (cf. fig. 4). A similar IR absorption band was also reported [40,41] for CO adsorbed on pure silicalite, and on non-porous silica [66]. Note that a weak IR absorption at about 2160 cm^{-1} is also present in the spectra corresponding to the highest CO dosis in fig. 3.

3.3. Adsorption of dinitrogen

The spectroscopic study of N_2 adsorption on the H-FeZSM-5 samples has completed and confirmed the characterization carried out by using CO as the IR spectroscopic probe. The effect of adsorbed N_2, at 77 K, on the O–H stretching region of the sample fired at 773 K is shown in fig. 6. The band corresponding to bridged OH groups (at 3630 cm^{-1}) is gradually eroded and shifted to 3530 cm^{-1} ($\Delta\nu = -100$ cm^{-1}) due to formation of hydrogen-bonded adducts, as depicted in scheme 3. A similar effect was reported for dinitrogen adsorbed on H-ZSM-5 [55,56], but the corresponding shift is in the -109 to -120 cm^{-1} range; this again is a reflection of the lower Brønsted acidity of the ferrisilicate.

Fig. 6 also shows that for high N_2 equilibrium pressure the bands due to silanols (3747 and 3720 cm^{-1}) are also partially eroded and shifted to 3715 and 3666 cm^{-1}, respectively. This effect is entirely analogous to what was stated for adsorbed CO. In the N–N stretching region a single band was observed at 2331 cm^{-1}, as shown in fig. 7. This band is assigned, in agreement with previous work on H-GaZSM-5 [33], to the N–N stretching of the OH···N≡N adduct depicted in scheme 3. It

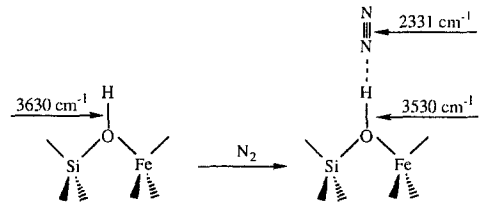

Scheme 3.

shows a hypsochromic shift $\Delta\nu = +10$ cm^{-1} with respect to the Raman-active fundamental stretching mode of dinitrogen adsorbed on silicalite, which was observed at 2321(±2) cm^{-1} [33]. This hypsochromic shift is the expected effect [56,67–69] of an end-on electrostatic interaction of N_2 with a positively charged centre, i.e. the acidic proton. The weak shoulder at ca. 2324 cm^{-1}, observable only at high N_2 equilibrium pressure, is assigned to the N–N stretching mode of SiOH···N_2 adducts.

Fig. 8 shows the effect of adsorbed dinitrogen on the O–H stretching region of the ferrisilicate sample fired at 973 K. Since Brønsted acid sites were eliminated during

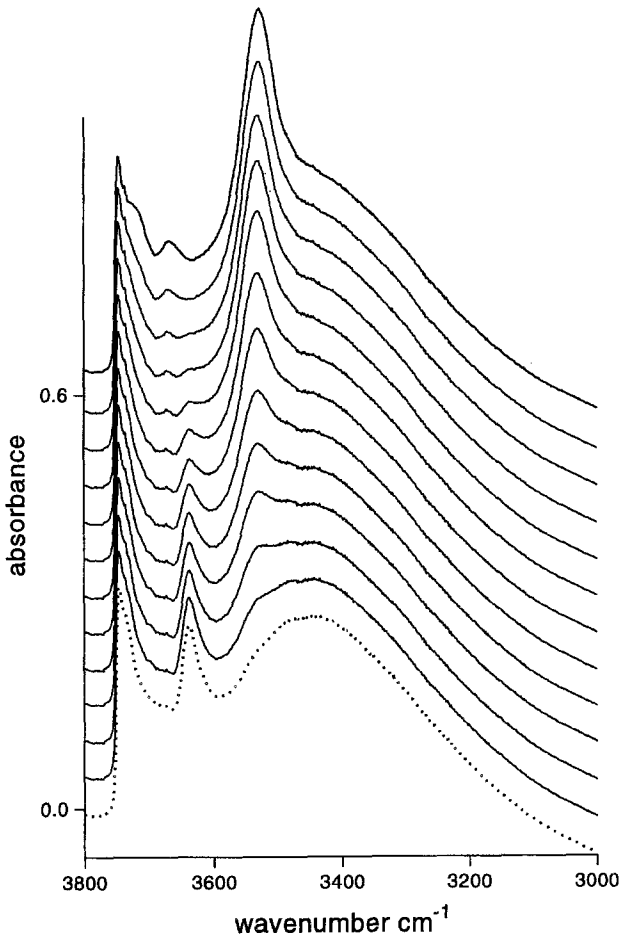

Fig. 6. As in fig. 2: dinitrogen adsorption at 77 K.

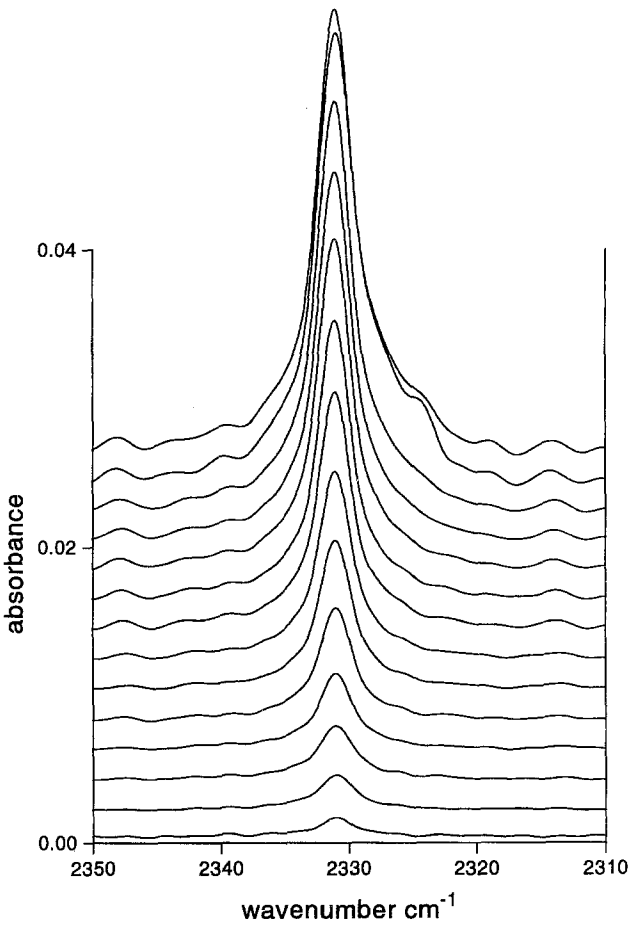

Fig. 7. Infrared spectra of dinitrogen adsorbed at 77 K and increasing equilibrium pressure (from ca. 10^{-2} to 40 Torr) on H-FeZSM-5 calcined at 773 K. All spectra were background subtracted.

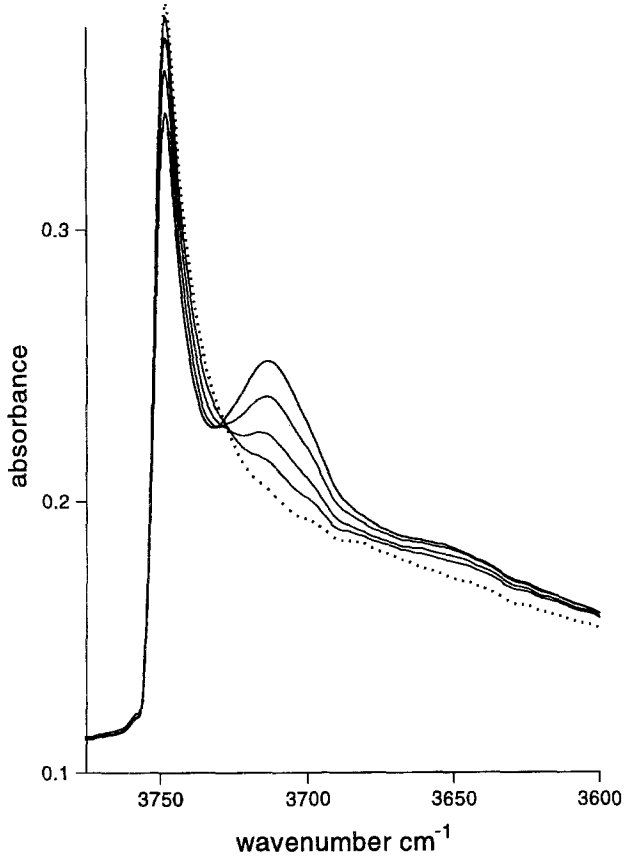

Fig. 8. As in fig. 4: dinitrogen adsorption at 77 K.

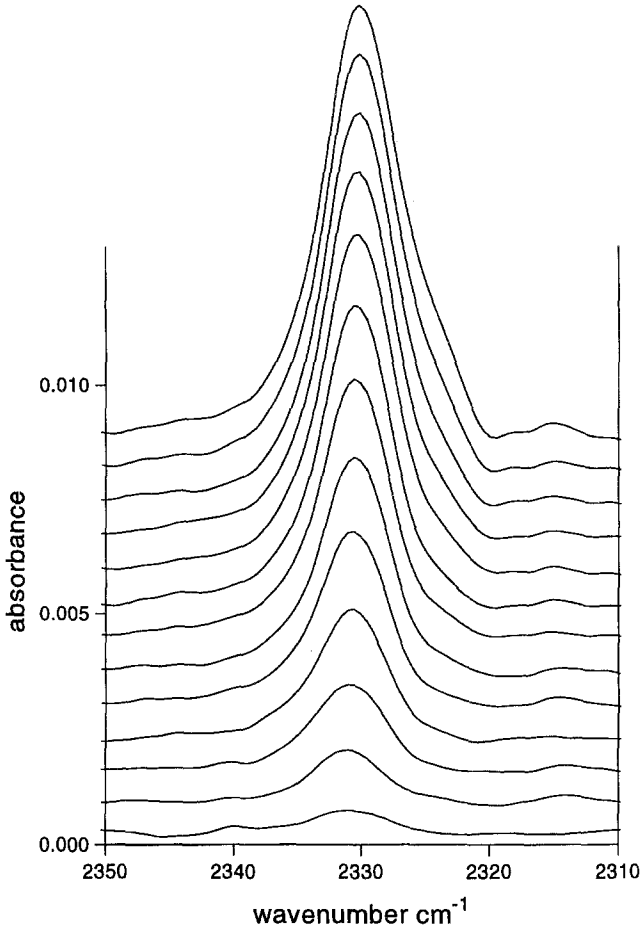

Fig. 9. Infrared spectra of dinitrogen adsorbed at 77 K and increasing equilibrium pressure (10^{-2} to 40 Torr) on H-FeZSM-5 calcined at 973 K.

thermal treatment, the only phenomenon observed is a partial erosion of the silanols band at 3747 cm^{-1} with attendant formation of a new broad band centred at 3713 cm^{-1}, which corresponds to the O–H stretching of hydrogen-bonded SiOH···N≡N adducts. Note the isobestic point at 3729 cm^{-1}. The corresponding N–N stretching mode is observed, in fig. 9, at 2324 cm^{-1}: low-frequency shoulder of the main IR absorption band.

For low N_2 equilibrium pressure, fig. 9 shows a main band centred at 2331 cm^{-1}, which is the same frequency observed for OH···N_2 adducts formed with Brønsted acid sites (cf. fig. 7). However, this is purely coincidental; it should be clear that this IR absorption band cannot be due to such adducts since Brønsted acid sites are no longer present, as shown in fig. 8 and also in the foregoing section on CO adsorption on the same zeolite sample. We assign the 2331 cm^{-1} band in fig. 9 to the N–N stretching of dinitrogen adducts formed with Fe^{3+} ions in extraframework iron oxide species, which were also revealed by CO adsorption: broad band at 2150–2190 cm^{-1} in fig. 5. Two facts must be stressed, (i) the 2331 cm^{-1} band (fig. 9) shifts to slightly lower wavenumbers ($\Delta\nu = -1.5$ cm^{-1}) at high N_2 equilibrium pressure, and (ii) it has a high-frequency tail. The small bathochromic shift observed upon increasing N_2 equilibrium pressure can be explained in terms of lateral interactions between N_2 molecules adsorbed in adjacent positions on extraframework iron oxide crystallites; by contrast, the band due to OH···N_2 adducts (fig. 7) was found to keep a constant frequency: 2331 cm^{-1} as expected for isolated hydroxyl groups (Brønsted acid sites). The high-frequency tail suggests a contribution from N_2 adsorbed on Fe^{3+} ions present at edges and corners of extraframework aggregates, as already discussed for CO adsorption.

Finally, a fruitful comparison can be made with the results of a recent study [33] on H-GaZSM-5 samples. Briefly, no significant loss of framework gallium was found for samples having a Si/Ga ratio of 50, even after heating at 973 K. For samples with Si/Ga = 25, extraframework gallium species were found which adsorbed dinitrogen giving a main IR absorption band at 2336.5 cm^{-1} (with shoulders in the 2340–2348 cm^{-1} range). Adsorbed CO gave rise to a main IR absorption band at 2200 cm^{-1}. When these results are compared with corresponding values found in the present work for N_2 and CO adsorbed on extraframework iron species: 2331 and 2174 cm^{-1}, respectively, it becomes clear that extraframework Fe^{3+} ions show a smaller polarizing power. Since Ga^{3+} and Fe^{3+} have nearly the same ionic radius, it is inferred that Fe^{3+} ions in extraframework species of

the ferrisilicate are less coordinatively unsaturated than corresponding Ga^{3+} ions in the gallosilicate analogue. From these facts two main conclusions can be drawn: (i) ferrisilicates have a lower thermal stability than gallosilicates, and (ii) extraframework species tend to form larger aggregates in the case of the ferrisilicates, thus leading to exposed metal ions which are less coordinatively unsaturated.

Note that formation of relatively large aggregates of extraframework iron oxide species in ferrisilicate samples having a very low (average) concentration of iron atoms (Si/Fe = 50) suggests a non homogeneous distribution of the metal ion in the zeolite framework. This would not be necessarily related to energy minimization in the ferrisilicate lattice [70–72]; it is more likely to reflect local heterogeneity in the parent gel.

Acknowledgement

We thank Dr. G. Petrini (ENICHEM) for the generous gift of a ferrrisilicate sample. AZ thanks the Spanish Ministerio de Educación y Ciencia (DGICYT) for a sabbatical stay at the Universidad de las Islas Baleares.

References

[1] W. Hölderich, M. Hesse and F. Näumann, Angew. Chem. Int. Ed. Engl. 27 (1988) 226.
[2] P.B. Venuto, Microporous Mater. 2 (1994) 297.
[3] R. Szostak and T.L. Thomas, J. Chem. Soc. Chem. Commun. (1986) 113.
[4] P. Ratnasamy, A.N. Kothastane, V.P. Shiralkar, A. Thangaraj and S. Ganapathy, in: *Zeolite Synthesis*, ACS Monograph No. 398, eds. M.L. Occelli and H.E. Robson (Am. Chem. Soc. Washington, 1989) p. 405.
[5] C.V.A. Duke, K. Latham and C.D. Williams, Zeolites 15 (1995) 213.
[6] A.J. Chandwadkar, R.N. Bhat and P. Ratnasamy, Zeolites 11 (1991) 42.
[7] L. Marosi, J. Stabenow and M. Schwarzmann, German Patent Appl. 2831611 (1980).
[8] R. Szostak and T.L. Thomas, J. Catal. 100 (1986) 555.
[9] R. Szostak, V. Nair and T.L. Thomas, J. Chem. Soc. Faraday Trans. I 83 (1987) 487.
[10] G. Doppler, R. Lehnert, L. Marosi and A.X. Trautwein, Stud. Surf. Sci. Catal. 37 (1988) 215.
[11] A. Meagher, V. Nair and R. Szostak, Zeolites 8 (1988) 3.
[12] G.P. Handreck and T.D. Smith, J. Chem. Soc. Faraday Trans. I 85 (1989) 3195.
[13] J.G. Ulan, R. Gronsky and R. Szostak, Zeolites 11 (1991) 466.
[14] R. Szostak, *Molecular Sieves* (Van Nostrand Reinhold, New York, 1989).
[15] P. Ratnasamy and R. Kumar, Catal. Today 9 (1991) 328.
[16] P. Ratnasamy and R. Kumar, Catal. Lett. 22 (1993) 227.
[17] A. Brückner, R. Lück, W. Wieker, B. Fahlke and H. Mehner, Zeolites 12 (1992) 380.
[18] J. Patarin, H. Kessler and J.L. Guth, Zeolites 10 (1990) 674.
[19] D.M. Bibby and M.P. Dale, Nature 317 (1985) 157.
[20] Q. Huo, S. Feng and R. Xu, J. Chem. Soc. Chem. Commun. (1988) 1486.
[21] A. Hagen, F. Roessner, I. Weingart and B. Spliethoff, Zeolites 15 (1995) 270.
[22] D.H. Lin, G. Coudurier and J.C. Vedrine, Stud. Surf. Sci. Catal. 49 (1989) 1431.
[23] G. Vorbeck, M. Richter, R. Fricke, B. Parlitz, E. Screier, K. Szulmewsky and B. Zibrowius, Stud. Surf. Sci. Catal. 65 (1991) 631.
[24] J. Cejka, B. Wichterlova, J. Krtil, M. Krivanek and R. Fricke, Stud. Surf. Sci. Catal. 69 (1991) 347.
[25] G.I. Panov, G.A. Sheveleva, A.S. Kharitonov, V.N. Romannikov and L.A. Vostrikova, Appl. Catal. A 82 (1992) 31.
[26] J. Ho Kim, S. Namba and T. Yashima, Appl. Catal. A 83 (1993) 51.
[27] V.I. Sobolev, G.I. Panov, A.S. Kharitonov, V.N. Romannikov, A.M. Volodin and K.G. Ione, J. Catal. 139 (1993) 435.
[28] V.I. Sobolev, A.S. Kharitonov, O.V. Panna and G.I. Panov, Stud. Surf. Sci. Catal. 98 (1995) 159.
[29] R. Szostak, V. Nair, D.K. Simmons, T.L. Thomas, R. Kuvadia, B. Dunson and D.C. Shieh, Stud. Surf. Sci. Catal. 37 (1988) 403.
[30] K. Yogo, S. Tanaka, T. Ono, T. Mikami and E. Kikuchi, Microporous Mater. 3 (1994) 39.
[31] E. Kikuchi, K. Yogo, S. Tanaka and M. Abe, Chem. Lett. (1991) 1063.
[32] I. Inui, S. Iwamoto, S. Kojo and T. Yoshida, Catal. Lett. 13 (1992) 87.
[33] C. Otero Areán, G. Turnes Palomino, F. Geobaldo and A. Zecchina, J. Phys. Chem. 100 (1996) 6678.
[34] A. Zecchina and C. Otero Areán, Chem. Soc. Rev., in press.
[35] F. Geobaldo, C. Lamberti, G. Ricchiardi, S. Bordiga, A. Zecchina, G. Turnes Palomino and C. Otero Areán, J. Phys. Chem. 99 (1995) 11167.
[36] S. Bordiga, F. Geobaldo, C. Lamberti, A. Zecchina, F. Boscherini, F. Genoni, G. Leofanti, G. Petrini, M. Padovan, S. Geremia and G. Vlaic, Nucl. Instr. Meth. Phys. Res. B 97 (1995) 23.
[37] S. Bordiga, R. Buzzoni, F. Geobaldo, C. Lamberti, E. Giamello, A. Zecchina, G. Leofanti, G. Petrini, G. Tozzola and G. Vlaic, J. Catal. 158 (1996) 486.
[38] M. Tamarasso, B. Perego and B. Notari, US Patent 4410501 (1983).
[39] W.M. Meier and D.H. Olson, *Atlas of Zeolite Structure Types* (Butterworths, London, 1987).
[40] A. Zecchina, S. Bordiga, G. Spoto, L. Marchese, G. Petrini, G. Leofanti and M. Padovan, J. Phys. Chem. 96 (1992) 4991.
[41] A. Zecchina, S. Bordiga, G. Spoto, D. Scarano, G. Petrini, G. Leofanti, M. Padovan and C. Otero Areán, J. Chem. Soc. Faraday Trans. 88 (1992) 2959.
[42] P.A. Jacobs and R. von Ballmoos, J. Phys. Chem. 86 (1982) 3050.
[43] M.B. Sayed, R.A. Kydd and R.P. Cooney, J. Catal. 88 (1984) 137.
[44] G. Qin, L. Zheng, Y. Xie and C. Wu, J. Catal. 95 (1985) 609.
[45] L.M. Kustov, V.B. Kazansky, S. Beran, L. Kubelková and P. Jiru, J. Phys. Chem. 91 (1987) 5247.
[46] J. Datka, M. Bozcar and P. Rymarowicz, J. Catal. 114 (1988) 368.
[47] J. Dwyer, Stud. Surf. Sci. Catal. 37 (1988) 333.
[48] R. Borade, A. Sayari, A. Adnot and S. Kaliaguine, J. Phys. Chem. 94 (1990) 5989.
[49] C.T.W. Chu and C.D. Chang, J. Phys. Chem. 89 (1985) 1569.
[50] J. Datka and T. Abramowicz, J. Chem. Soc. Faraday Trans. 90 (1994) 2417.
[51] I. Mirsojew, S. Ernst, J. Weitkamp and H. Knözinger, Catal. Lett. 24 (1994) 235.
[52] A.Yu. Khodakov, L.M. Kustov, T.N. Bondarenko, A.A. Dergachev, V.B. Kazansky, Kh.M. Minachev, G. Borbély and H.K. Beyer, Zeolites 10 (1990) 603.

[53] D.J. Parrillo, C. Lee, R.J. Gorte, D. White and W.E. Farneth, J. Phys. Chem. 99 (1995) 8745.
[54] G.C. Pimentel and A.L. McClellan, *The Hydrogen Bond* (Freeman, San Francisco, 1960) ch. 3.
[55] F. Wakabayashi, J.N. Kondo, K. Domen and C. Hirose, J. Phys. Chem. 99 (1995) 10573; J. Phys. Chem. 100 (1996) 4154.
[56] K.M. Neyman, P. Strodel, S.Ph. Ruzankin, N. Schlensog, H. Knözinger and N. Rösch, Catal. Lett. 31 (1995) 273.
[57] M.A. Makarova, K.M. Al-Ghefaili and J. Dwyer, J. Chem. Soc. Faraday Trans. 90 (1994) 383.
[58] H. Berndt, A. Martin, H. Kosslick and B. Lücke, Microporous Mater. 2 (1994) 197.
[59] M.S. Stave and J.B. Nicholas, J. Phys. Chem. 99 (1995) 15046.
[60] S. Bordiga, D. Scarano, G. Spoto, A. Zecchina, C. Lamberti and C. Otero Areán, Vib. Spectrosc. 5 (1993) 69.
[61] S. Bordiga, C. Lamberti, F. Geobaldo, A. Zecchina, G. Turnes Palomino and C. Otero Areán, Langmuir 11 (1995) 527.
[62] A. Zecchina, D. Scarano and A. Reller, J. Chem. Soc. Faraday Trans. I 84 (1988) 2327.
[63] A. Raj and S. Sivasanker, J. Catal. 147 (1994) 207.
[64] E. Guglielminotti, J. Phys. Chem. 98 (1994) 4884.
[65] S. Bordiga, E. Escalona Platero, C. Otero Areán, C. Lamberti and A. Zecchina, J. Catal. 137 (1992) 179.
[66] G. Ghiotti, E. Garrone, C. Morterra and F. Boccuzzi, J. Phys. Chem. 83 (1979) 2863.
[67] H. Böse and H. Förster, J. Mol. Struct. 218 (1990) 393.
[68] L. Koubi, M. Blain, E. Cohen de Lara and J.M. Leclerq, Chem. Phys. Lett. 217 (1994) 544.
[69] D.M. Bishop and S.M. Cybulski, Chem. Phys. Lett. 230 (1994) 177.
[70] D.W. Lewis, C.R.A. Catlow, G. Sankar and S.W. Carr, J. Phys. Chem. 99 (1995) 2377.
[71] D.W. Lewis, G. Sankar, C.R.A. Catlow, S.W. Carr and J.M. Thomas, Nucl. Instr. Meth. Phys. Res. B 97 (1995) 44.
[72] R.G. Bell, D.W. Lewis and C.R.A. Catlow, Stud. Surf. Sci. Catal. 98 (1994) 234.